Practical Introduction to LTE Radio Planning

J. Salo, M. Nur-Alam, K. Chang

This paper reviews basics of radio planning for 3GPP LTE. Both coverage-limited and interference-limited scenarios are considered. For the coverage-limited scenario LTE link budget is compared to that of 3GPP Release 8 HSPA+ with 2x2 MIMO. It is shown that, given the same 5MHz bandwidth, both systems have similar cell ranges but, for a given target bit rate, there exists an optimum LTE system bandwidth that maximizes cell range in both uplink and downlink. For the interference-limited scenario (with random uncoordinated interference) we illustrate the relationship between average network load, cell edge target throughput and cell range, as well as the notion of interference margin for cell range dimensioning. Impact of base station antenna configurations on dual-stream Multiple-Input Multiple-Output (MIMO) performance is demonstrated by means of a real-world measurement example. The impact of advanced LTE radio resource management features are briefly reviewed. Finally, the most important radio parameter planning tasks are introduced.

1. INTRODUCTION

This paper introduces LTE from the perspective of radio network planning. The paper is mainly targeted for readers with earlier experience in radio planning and mobile communications. Some prior knowledge of radio engineering and LTE is assumed as principles of OFDMA and SC-FDMA, as described in 3GPP LTE specifications, will not be reviewed in this paper. Instead the reader is referred to well-known literature references [1–3]. The most important LTE radio interface parameters are summarized in Table 1 for the convenience of the reader. Our focus is on the FDD variant of LTE, although most of the discussion is also applicable to TDD.

Abbreviations

BCCH	Broadcast Channel
CQI	Channel Quality Indicator
FDD	Frequency Division Multiplexing
HARQ	Hybrid Automatic Repeat Request
HS-DSCH	HSDPA Downlink Shared Channel
LTE	Long Term Evolution
PCI	Physical Cell Identity
PDCCH	Physical Downlink Control Channel
PDSCH	Physical Downlink Shared Channel
PMI	Precoder Matrix Indicator
PRACH	Physical Random Access Channel
PRB	Physical Resource Block
PUSCH	Physical Uplink Shared Channel
RS	Reference Signal
SINR	Signal-to-Interference-Noise-Ratio
TDD	Time Division Multiplexing
TTI	Transmission Time Interval

Table 1
Summary of main LTE radio interface parameters

Quantity	LTE DL	LTE UL
System bandwidth	1.4, 3, 5, 10, 15, 20MHz	1.4, 3, 5, 10, 15, 20MHz
Multiple access	OFDMA	single carrier FDMA
Cyclic prefix	4.7 microsec / 16.7 microsec	4.7 microsec / 16.7 microsec
Modulation	QPSK, 16QAM, 64 QAM	QPSK, 16QAM (64 QAM for Cat5 UE)
Channel coding*	turbo coding	turbo coding
HARQ	8 processes, up to 7 retransm./proc	8 processes
Power control	none$^\natural$	cell-specific and UE-specific
Handover	hard, network-triggered	hard, network-triggered
Num of Tx antennas	$1, 2, 4$ ‡	1 $^\sharp$
Num of Rx antennas	arbitrary	≥ 2
Transmit diversity	Space-Frequency Block Code	transmit antenna selection diversity
Beamforming	3GPP codebook or proprietary	none
Spatial multiplexing	open-loop, closed-loop	none†
PRB allocation per TTI	distributed or contiguous	contiguous$^\flat$

$\star$ For PDSCH and PUSCH. For L1/L2 control and common channels other coding schemes can be used.
$\natural$ Downlink Only static Reference Signal power boosting has been specified by 3GPP, vendor-specific implementations possible.
‡ With UE-specific reference signals (vendor-specific beamforming) arbitrary number of Tx antennas.
♯ For simultaneous transmission. Transmit antenna selection is possible with RF switching.
† Multiuser MIMO possible in UL in 3GPP Release 8.
$\flat$ Intra-TTI and inter-TTI frequency hopping is possible in UL.

2. LTE COVERAGE IN NOISE-LIMITED SCENARIO

2.1. Definition of average SINR

Probably the most useful performance metric for LTE radio planner is the average signal-to-interference-and-noise ratio, SINR_{ave}, defined as

$$\mathrm{SINR}_{ave} = \frac{S}{I+N}\,, \tag{1}$$

where S is the average received signal power, I is the average interference power, and N is the noise power. In measurement and simulation analysis, the sample averages should be taken over small-scale fading of S and I and over a large number of HARQ retransmissions (several hundreds of TTIs, preferably). The average interference power can be further decomposed as

$$I = I_{own} + I_{other}\,, \tag{2}$$

where I_{own} and I_{other} are the average own-cell and other-cell interference power. In case of HSPA, $I_{own} = (1-\alpha)P_{own}$ with $\alpha \in [0,1]$ denoting the average channel multipath orthogonality factor and P_{own} denoting the own-cell transmit power. In LTE, orthogonality is often assumed unity for simplicity, even though in reality the following nonidealities may result in non-negligible own-signal interference in LTE:

- Inter-symbol interference due to multipath power exceeding cyclic prefix length
- Inter-carrier interference due to Doppler spread (large UE speed)

- Transmit signal waveform distortion due to transmitter nonlinearities, measured in terms of Error Vector Magnitude

In both LTE and HSPA the effective value of α depends on the multipath characteristics and receiver implementation. For HSDPA with receiver equalizer, $\alpha > 0.9$ can be assumed in most cases. In this paper, $\alpha = 1$ is assumed for LTE and hence $I_{own} = 0$. The impact of $\alpha < 1$ can be seen only at high SINR_{ave}; at low SINR_{ave} noise power dominates the denominator of (1) over interference power, for both HSDPA and LTE.

In the remainder of the paper, we drop the subscript and denote average signal-to-interference-ratio simply with SINR.

2.2. LTE versus HSPA+ coverage in noise-limited scenario

In Table 2 link budgets of LTE and HSPA+ are compared. Both systems have 5 MHz system bandwidth, 2Tx $\times$ 2Rx MIMO antenna system, and equal antenna and RF characteristics for fair comparison. Note that the link budget is carrier-frequency independent, as it is given in terms of maximum path loss, not cell range. A single cell in isolation is assumed, i.e., no interference ($I = 0$).

The following differences in link budgets can be seen:

- In HSDPA, L1/L2 control and pilot channel overhead is a fraction of the total downlink transmit power (typically about 20%). In LTE, L1/L2 control channels consume a fraction of DL OFDM symbols, 30% overhead in time/frequency resource element usage is assumed in Table 2, corresponding to three symbols wide L1/L2 control channel region.

- For a given bit rate target, required SINR is slightly different for LTE and HSPA+. However, in the noise-limited regime the difference in target SINR is typically small, less than 2 dBs.

- The noise bandwidth is about 5MHz for HSPA+ UL and DL, as well as LTE DL. For LTE UL, however, the noise bandwidth depends on the number of allocated physical resource blocks (frequency allocation), since symbols are detected in time-domain and noise is accumulated only over the actual occupied bandwidth.

While HSPA+ and LTE have similar performance in terms of coverage, the same is not true for system-level capacity under network interference, where LTE has advantage over HSPA+ due to more advanced radio features, such as multiuser-MIMO, frequency-domain scheduling and inter-cell interference coordination.

2.3. Optimizing LTE system bandwidth for coverage

In this section it is shown that, for a given target bit rate, there is an optimum system bandwidth in DL and UL in terms of maximizing coverage. Of course, typically other decision criteria besides coverage come into play when choosing system bandwidth for practical network deployment. The purpose of the following discussion is mainly to illustrate trade-off between bandwidth and coverage in LTE uplink and downlink.

Downlink (Fig. 1): Consider a fixed rate of information transmission for a fixed transmit power. As the number of allocated Physical Resource Blocks (PRBs) becomes larger, code rate decreases and channel coding gain in turn increases. Therefore, for a fixed DL system bandwidth it pays off to use as many PRBs as possible to minimize required SINR[1]. On the other hand, if one is allowed to use the system bandwidth as a design parameter, there exists an optimum system bandwidth for a given target bit rate. This is due to the fact that, assuming fixed total transmit power, transmit power per PRB (power density) increases as system bandwidth is reduced. This is illustrated in Figure 1. For bit

[1]One PRB is a contiguous chunk of 12 subcarriers, or 180kHz, in frequency domain.

Table 2
Link budget comparison in noise-limited scenario, a single user at cell edge for 2x2 LTE and 2x2 HSPA+, 5 MHz LTE bandwidth. Target bit rate: 1Mbps DL, 128Mbps UL.

Quantity	LTE DL	HSDPA	LTE UL	HSUPA
Transmit power*	46 dBm	45 dBm$^\flat$	23 dBm†	24 dBm
Antenna + feeder gain	15 dB	15 dB	-3 dB	-3 dB
MHA gain	-	-	2 dB	2 dB
Rx Noise Figure	7 dB	7 dB	2 dB	2 dB
SNR target	-4 dB‡	-5 dB‡	-12 dB‡	-13 dB$^\diamondsuit$
RX sensitivity	-105 dBm$^\sharp$	-105 dBm	-117 dBm	-118 dBm
Max path loss	164 dB	163 dB	154 dB	156 dB

$\star$ Sum power of two transmit antennas
$\flat$ max HS-DSCH power 42 dBm per antenna
† Category 3 LTE terminal
‡ All bandwidth allocated for the single user in DL and UL.
$\diamondsuit$ E_b/N_0 target of 2dB for 128 kbps, processing gain of 15 dB .
$\sharp$ UL and DL noise bandwidth is 5MHz.

rate target of 128 kbps, the optimum bandwidth is 1.4 MHz, while for 512 kbps and 1Mbps target bit rate, it is 3 and 5MHz, respectively.

Uplink (Fig. 2): There is an optimum system bandwidth in the uplink, too, as illustrated in Figure 2. The difference to downlink is that the noise bandwidth equals actual instantaneous scheduled UL bandwidth, which may be less than the system bandwidth. From Fig. 2, it can be seen that for bit rates $\leq$ 256kbps the optimum number of PRBs is about $3-5$, meaning that 1.4MHz system bandwidth (6 PRBs) would be sufficient for optimal coverage. For bit rates above 2Mbps, system bandwidth of 5MHz or more is needed in order for system bandwidth not to limit receive sensitivity (UL coverage).

In practice, control and common channel coverage should be taken into account, too. Simulation results in [1] indicate that for low bit rate services uplink random access channel coverage may be the limiting factor, instead of the PDSCH/PUSCH considered here.

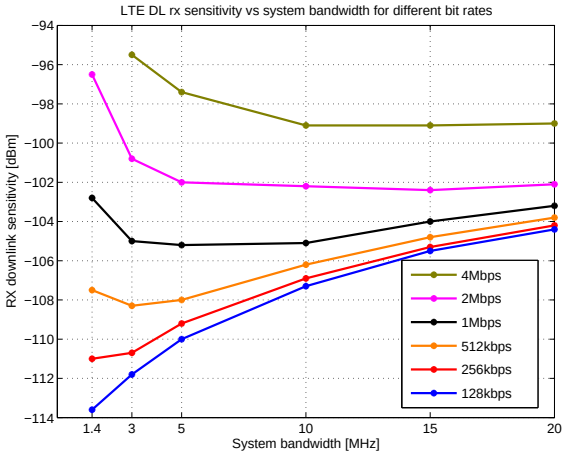

Figure 1. LTE downlink sensitivity versus system bandwidth for different bitrates, channel unaware scheduling. Total system bandwidth is allocated to a single user.

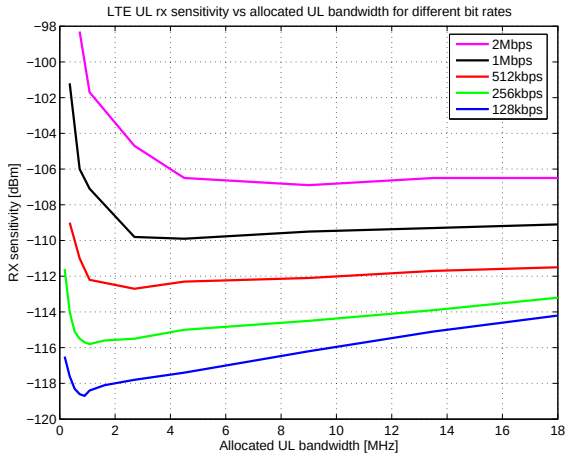

Figure 2. LTE uplink sensitivity versus allocated bandwidth for different bitrates, channel unaware scheduling.

3. LTE IN INTERFERENCE-LIMITED SCENARIO

A somewhat simplified engineering view on SINR under non-negligible other cell interference is presented in this section. In particular, interference is here characterized only by its average power, whereas (as in HSDPA) it is in fact very bursty when examined at TTI level. Therefore, the interplay of HARQ and interference (traffic) time correlation is completely neglected in the sequel, for the sake of potential radio planning insights.

3.1. SINR under random (uncoordinated) interference

At cell edge, the interference from K neighbouring cells can be written as ($I = I_{other}$)

$$I = \sum_{k=1}^{K} \gamma_k I_{max,k} \quad (3)$$

$$= \gamma I_{max}\,, \quad (4)$$

where $I_{max} = \sum_{k=1}^{K} I_{max,k}$ is the maximum interference power at cell edge, and γ_k is the subcarrier activity factor of the kth cell. We assume that the average cell load is equal for all cells, in other words, $\gamma_k = \gamma$, for all k.

Signal-to-Interference-and-Noise ratio can be written as a function of SNR, SIR and cell load γ as

$$\mathrm{SINR} = \frac{S}{I+N} \quad (5)$$

$$= \frac{S}{\gamma I_{max} + N} \quad (6)$$

$$= \frac{1}{\frac{\gamma}{\mathrm{SIR}_{min}} + \frac{1}{\mathrm{SNR}}}\,, \quad (7)$$

where $\mathrm{SIR}_{min} = \frac{S}{I_{max}}$ and $\mathrm{SNR} = \frac{S}{N}$. We again emphasize that all quantities are average values, where the averaging is over small-scale fading of S and I. The value of SIR_{min} depends on network geometry and antenna configuration (but not on cell range) and is in practice determined from system simulations or network measurements. Typical values are $\mathrm{SIR}_{min} = -4\ldots-1$dB. The interference is here implicitly modelled as Gaussian noise, as is the common practice. It always applies that $\mathrm{SINR} < \gamma^{-1}\mathrm{SIR}_{min}$ and $\mathrm{SINR} < \mathrm{SNR}$. Therefore, without inter-cell interference coordination or intelligent channel-aware scheduling, throughput is limited by other-cell interference.

The relation of SINR and SNR is shown in Fig. 3 for different values of network load, γ. It can be seen that even a low network load will saturate SINR, and hence throughput.

3.2. Link budget with non-negligible interference: Interference Margin

The link budget in Table 2 assumed that interference power is negligible, i.e., $\mathrm{SNR} \gg \frac{\mathrm{SIR}_{min}}{\gamma}$ in Eq. (7). When this is not the case, target SNR in the noise-limited link budget must be substituted with a modified SNR target

$$\mathrm{SNR}_{\mathrm{intf}} = \mathrm{SINR} + \mathrm{NR}\,, \qquad [\mathrm{dB}] \quad (8)$$

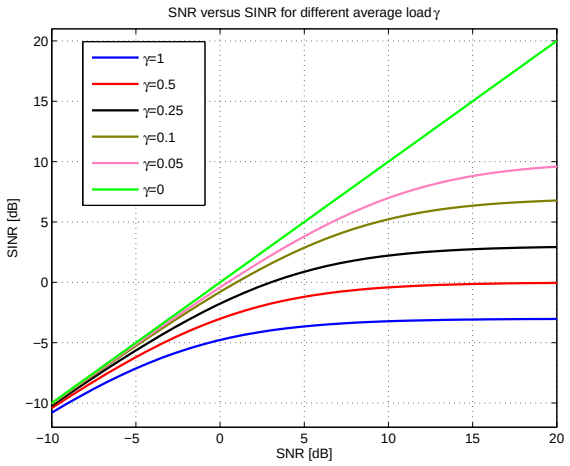

Figure 3. Cell edge SINR versus SNR for different network average loads (γ), $\text{SIR}_{min} = -3$ dB.

where NR denotes noise power rise due to interference, and SINR is determined by the throughput target. Cell range can then be solved in the usual manner from SNR_{intf} where the received signal power, S, is a function of path loss (cell range) and effective isotropic transmit power. What remains to be done is to obtain an expression for the noise rise. Before doing so, it is useful to note, again, that SINR can at cell edge never exceed $\frac{\text{SIR}_{min}}{\gamma}$ in Eq. (7). As $\text{SINR} \to \frac{\text{SIR}_{min}}{\gamma}$, SNR must in turn increase in order to keep SINR less than its upper limit. Therefore, one sees that the noise rise in Eq. (8) will be huge when the target SINR approaches $\frac{\text{SIR}_{min}}{\gamma}$, hence drastically shrinking the cell size.

Graphically, the same concept can be seen in Fig. 3 where the noise rise is the difference between the noise-limited case ($\gamma = 0$) and loaded case, see Eq. (8). For example, with 100% load the noise rise is 23dB at SNR = 20dB. As SINR approaches $\text{SIR}_{min} = -3$ dB, large increase in SNR is required for diminishing gains in SINR, and therefore cell edge throughput.

To derive formula for the noise rise, we first define in linear scale

$$\text{NR} = \frac{I+N}{N} \quad (9)$$

$$= \frac{\text{SNR}}{\text{SINR}}. \quad (10)$$

Substituting, $\text{SNR} = \text{NR} \cdot \text{SINR}$ in Eq. (7) and solving for NR results in

$$\text{NR} = \frac{1}{1-\gamma\frac{\text{SINR}}{\text{SIR}_{min}}}. \quad (11)$$

Here SINR depends on the cell edge throughput target and SIR_{min} on the network geometry. One can see that noise rise is very steep near the pole $\text{SINR} = \frac{\text{SIR}_{min}}{\gamma}$. Therefore, it is increasingly difficult to reach the upper limit cell edge throughput.

3.3. Trade-off between cell range, network load and cell edge throughput

In this section we illustrate the relationship between the three basic network planning variables: cell range, average network load and cell edge throughput. Towards this end, we write

$$\text{SNR} = \frac{S}{N} \quad (12)$$

$$= \frac{\text{EIRP}}{LN}, \quad (13)$$

where EIRP is the effective isotropic radiated power, and L is the path loss, given in linear scale as

$$L = MAd^B. \quad (14)$$

Here A is the median path loss at one kilometer distance (depends on carrier frequency and propagation environment), B is the path loss exponent, d is the distance in kilometers and M is the shadow-fading margin.

In linear scale, SINR as a function of cell range d and network load γ is

$$\text{SINR} = \frac{1}{\frac{\gamma}{\text{SIR}_{min}} + \frac{MAd^B N}{\text{EIRP}}} \quad (15)$$

There is a one-to-one mapping between SINR and average throughput. Therefore, (15) describes the tradeoff between γ, d and throughput. In the sequel, the three two-variable special cases are considered.

In the sequel, path loss model is based on 3GPP system LTE system simulation specification according to $L[\text{dB}] = 128 + 37\log_{10}(d)$ [4]. Shadowing standard deviation is 8dB with shadowing margin of $M = 8.7$dB (95% single-cell area probability) and building penetration loss of 20 dB. Other parameters are as given in Table 2, except that system bandwidth is 10 MHz. The SINR-throughput mapping was simulated for a 2×2 transmit diversity system.

3.3.1. Cell range vs network load, fixed cell edge throughput

In Fig. 4, the relation of network load and cell range is shown for various values of cell edge throughput. As network load increases, the cell range decreases for fixed cell edge throughput.

3.3.2. Network load vs cell edge throughput, fixed cell range

In Fig. 5, the relation of network load and cell edge throughput is shown for various values of cell range. For our later discussion concerning inter-cell interference coordination, it is instructive to note that when cell range is small, cell edge throughput is sensitive to network load. For cell range of 0.5km, if one was able to reduce effective network load from 0.4 to 0.1 cell edge throughput would double from 6 Mbps to 12 Mbps. Such a reduction could be possible by applying interference coordination between neighboring cells, hence directing interference to other part of the frequency spectrum. This will be discussed further later in this paper.

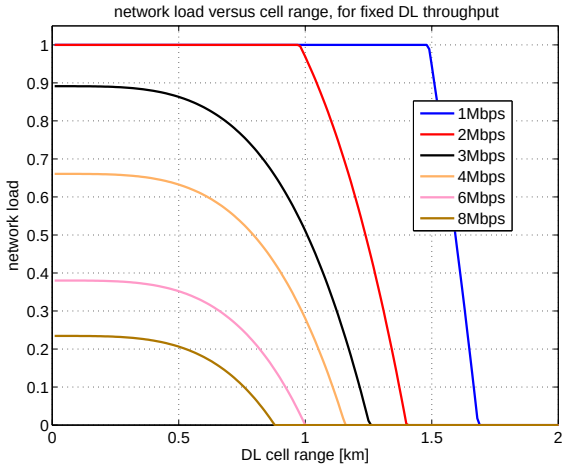

Figure 4. Network load versus cell range for fixed downlink cell edge throughput.

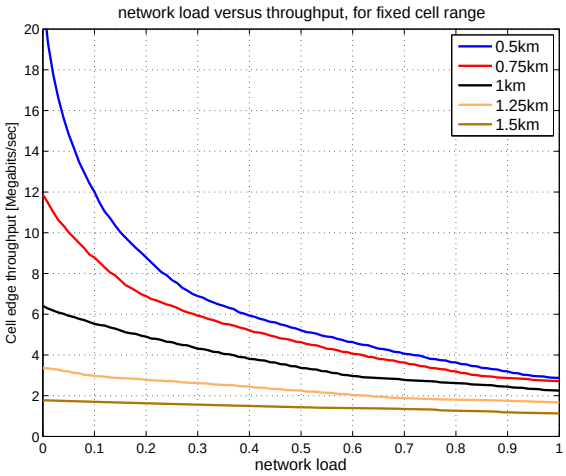

Figure 5. Network load versus cell edge throughput for fixed cell range.

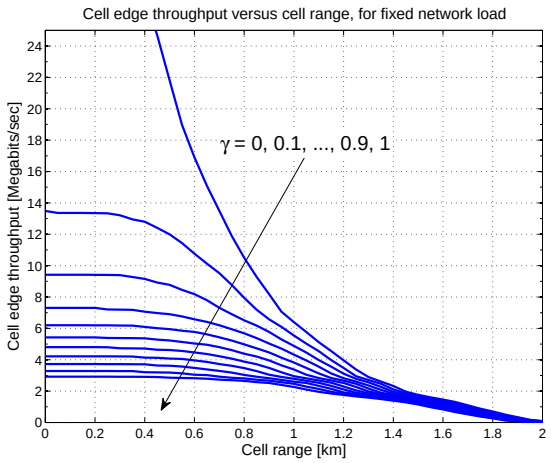

Figure 6. Cell range versus cell edge throughput for fixed network load.

3.3.3. Cell range versus cell edge throughput, fixed network load

In Fig. 6, the relation of cell range and cell edge throughput is shown for various values of network load. As the cell range increases, the cell edge throughput approaches the same limit regardless of cell load. Even the low network load of 10% limits throughput to less than 14Mbps by creating a noise floor from other-cell interference. It should be noted that downlink common channels and signals alone cause at least $>$ 10% network load over the $\approx$ 1 MHz bandwidth over which they are transmitted. On top of this, reference signals are transmitted over the entire system bandwidth. Sites in early FDD network implementations are not expected to be frame-synchronized, so that it is not possible to avoid inter-site interference by cleverly coordinating transmission in time and frequency.

4. MULTIPLE-INPUT MULTIPLE-OUTPUT (MIMO) CONFIGURATIONS

4.1. MIMO Transmission Schemes in LTE

While in common engineer talk there are appears to be several interpretations for the term, in this paper MIMO is taken to mean any radio interface that has at least two antennas at both ends, i.e., with this definition smallest MIMO antenna configuration would then be 2Tx $\times$ 2Rx. Note that in LTE all UEs are required to have two receive antennas, while the number of base station antennas can be[2] 1, 2, or 4. In principle, there are three ways to utilize MIMO antennas:

- *Combined transmit/receive diversity:* Normal two-branch diversity reception or transmission has the benefit of producing two copies of the same signal for reception, which with a suitable signal combining technique reduces fading variation. Similarly, a 2Tx $\times$ 2Rx antenna transmission results in reception of four signal replicas, with the corresponding additional reduction in fading. This version of MIMO is hence simply an enhanced diversity scheme, and as such is not by many considered "true" MIMO, since it does not actually increase transmission data rate. In LTE, space-frequency block coding based diversity scheme is used; this is an open-loop scheme where UE precoder feedback (PMI) is not required at the base station.

- *Beamforming:* This is very similar to the diversity transmission, the main nomenclatural difference being that in beamforming one typically considers a physical antenna beam being constructed towards the UE.

[2]With precoding using UE-specific reference signals ("beamforming") arbitrary number of antennas can be used. However, this transmission scheme is not expected to be supported in first vendor releases, due to hesitance from operators to deploy antenna arrays. The cell edge throughput gain from such configuration in rural/road environments would be substantial however, e.g., 9 dB from an 8-antenna panel array.

This requires closely spaced antennas, unlike the diversity schemes which require at least a few wavelength antenna spacing. Beamforming using 3GPP codebook also requires PMI feedback from UE. Mathematically, both beamforming and transmit diversity are both special cases of so-called rank-1 precoding[3]. LTE Rel 8 supports rank-1 precoding (or, "beamforming") using pre-defined 3GPP codebook (for 2 and 4 antennas), and any vendor-specific beamforming when using UE-specific reference signals (arbitrary number of base station antennas).

- *Spatial Multiplexing:* This is what many consider to be a true MIMO transmission scheme. With beamforming and diversity, base station transmits a single stream of information but uses the multiple antennas to either reduce fading (diversity) or increase signal power (beamforming). On the other hand, with 2Tx $\times$ 2Rx spatial multiplexing the idea is to transmit two parallel information streams over the same bandwidth, hence theoretically doubling the data rate and spectral efficiency. Both open-loop (only channel rank and CQI reported by UE) and closed-loop spatial multiplexing are supported (also precoding matrix information reported by UE). Delving slightly in implementation details, in LTE open-loop spatial multiplexing have been engineered in such a way that symbols in information streams are interleaved between the MIMO subchannels. Thus, the average SINR experienced by the transmitted symbols is the average of the two MIMO subchannels' SINRs. In uplink, spatial multiplexing is not supported for a single UE, but two different UEs are allowed to transmit at the same time; this is called multiuser-MIMO.

[3]In this paper, rank-1 precoding and beamforming are considered synonymous.

In practice, the choice of transmission scheme depends on instantaneous radio channel conditions and is adapted continuously. The main difference to non-MIMO transmission that, in addition to SINR, now also the channel rank has to be considered, since spatial multiplexing is feasible only if the instantaneous radio channel (during 1ms TTI) supports transmission of more than one information stream, or in terms of matrices, the 2Tx $\times$ 2Rx matrix channel's condition number and SINR are good enough. As a rule of thumb, in a spatially uncorrelated channel spatial multiplexing becomes useful when SINR $>$ 10 dB. Looking at Fig. 3 one can see that this requires very low network load for spatial multiplexing to work at cell edge, assuming that other-cell interference is uncoordinated.

4.2. Benefit of MIMO

The benefits of different MIMO schemes in downlink are roughly as follows:

Transmit/receive diversity: Compared to 1Tx $\times$ 1Rx the gain of 2Tx $\times$ 2Rx is about $6-7$ dB due to following factors: i) transmit power is doubled by adding another amplifier (3dB); ii) average received signal power is doubled because of two-antenna reception (3dB); iii) diversity from four signal paths brings additional gain which however strongly depends on the propagation environment (here pessimistically assumed $0-1$dB, higher gains are possible).

Rank-1 precoding: For slow-moving UEs the gain from closed-loop transmit diversity is $1-2$ dB higher than with the open-loop transmit/receive diversity. For fast-moving mobiles this improvement over diversity diminishes, or goes negative, since the CQI feedback cannot track the channel fast enough.

Spatial multiplexing: This scheme does not improve link budget, but increases data rate. With two antennas and an ideal MIMO radio channel, the data rate would be doubled. In practice, gains are considerably smaller due to the fact that for ideal operation the SINR of the two parallel subchannels should be high enough to support the same modulation and coding scheme.

This is very rarely the case, and the second stream must be transmitted at lower information bit rate. This point is further illustrated in the following subsection.

4.3. Example of Measured MIMO Radio Channel

Spatial multiplexing transmission is feasible only at those time instants when the radio channel conditions are favorable. There exist a wealth of literature on the theory of MIMO communication systems, and the interested reader is referred to the references. From radio planning point of view, the 2Tx $\times$ 2Rx MIMO channel power response λ at any given time instant can be written, on a subcarrier, as[4] $\lambda = \lambda_1 + \lambda_2$, where λ_1 and λ_2 are the power responses of the first and second MIMO subchannels, respectively. Each of the subchannels carries one information stream. As with a normal non-MIMO channel, the powers of the subchannels experience signal fading. If the power of the weaker subchannel, say λ_2, is very weak, the second information stream should not be transmitted at that time instant, since it will either be buried in noise, or alternatively, from link adaptation point of view, it is more spectrally efficient to transmit one stream with higher-order modulation and/or less channel coding. In either case, usage of spatial multiplexing depends on the instantaneous channel conditions which are reported to, and tracked, by the base station. When the second subchannel is weak, the channel is said to have "rank one", and spatial multiplexing is not used[5].

Fig. 7 presents an example of a narrowband measurement of a 2Tx $\times$ 2Rx channel in an urban environment at 2.1 GHz carrier frequrency. Two base station antenna configurations are shown: i) two vertically polarized transmit antennas at 3 wavelength separation (| |); ii) two cross-polarized transmit antennas at 0 deg and 90 deg angles (+). The dual-branch UE antenna is a realistic terminal microstrip antenna integrated in the terminal chassis, whose branch polarizations are not well-defined, as is typically the case for small integrated antennas. The figure shows the powers of the two MIMO subchannels as a function of travelled distance. Roughly in the midpoint of the measurement route the UE enters line-of-sight and the signal power of the stronger stream (λ_1) increases. The second stream power behaves differently for the two antenna setups. With the cross-polarized antenna base station setup the second stream (λ_2) is about 15 dB weaker than the stronger one. In contrast with the vertically polarized antennas the second stream is about 30 dB weaker. Thus, if the channel SINR is 20 dB, with the cross-polarized configuration the first stream SINR would be almost 20dB while the second stream would experience about SINR $\approx$ 5 dB which would still allow fairly high bit rate transmission over the second MIMO subchannel. However, with the vertically polarized antennas the second stream would be SINR ≈ -10 dB, which would not support high-rate transmission of the second stream.

Fig. 8 illustrates the same measurement routes using two different figures of merit, namely the total MIMO channel power response and ratio of MIMO subchannel powers, $\frac{\lambda_1}{\lambda_2}$. From the upper subplot it can be seen that the total power responses of the two antenna setups are slightly different. Vertically polarized configuration has almost negligibly higher received power in the line-of-sight, while the cross-polarized configuration, in turn, has slightly better power response in non-line-of-sight. From the lower subplot we note that the cross-polarized antenna setup has advantage in terms of the second subchannel power in line-of-sight conditions; the second subchannel is about 10 dB weaker than the first, compared to the 30 or so dBs for the vertically polarized case.

[4]The symbol λ is used here for historical reasons, since the MIMO subchannel power is related to the eigenvalues of the MIMO radio channel.

[5]Mathematically, the rank of the 2Tx $\times$ 2Rx channel is practically always two, so this terminology is strictly speaking a misnomer.

Summarizing the main radio planning message from the two figures:

- Dual-stream transmission is only feasible when the SINR of the second subchannel is high enough. This depends on the total channel SINR and the ratio of the subchannel powers.
- Base station antenna configuration has impact on the spatial multiplexing performance in two respects: total received signal and spatial multiplexing gain.
- In terms of total received signal power, the two compared antenna configurations are roughly equal with slight advantage for v-pol in line-of-sight, and vice versa in non-line-of-sight.
- In terms of spatial multiplexing gain, x-pol has large advantage in line-of-sight. There is no noticeable difference in non-line-of-sight.

The results indicate that cross-polarized base station antenna configuration should be favored when usage of spatial multiplexing is desired, as it offers more robust performance in all channel conditions. While these conclusions are in this paper illustrated by means of a single measurement example, similar conclusions have been drawn from large channel measurement campaigns reported in literature [5].

5. RADIO RESOURCE MANAGEMENT FEATURES

So far, we have discussed a simple "baseline" LTE radio configuration, assuming fully random (uncoordinated) interference and no special radio resource management features. The LTE radio interface specification Release 8 supports several advanced air interface functionalities that potentially improve network performance in certain environments. These are explained in the following.

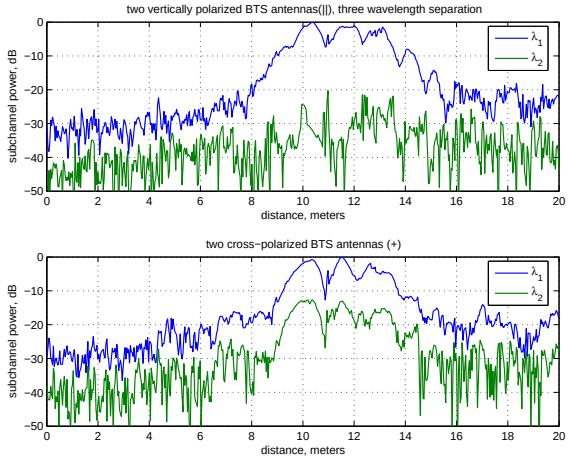

Figure 7. Example of measured MIMO radio channel, power response of the MIMO subchannels for two base station antenna configurations.

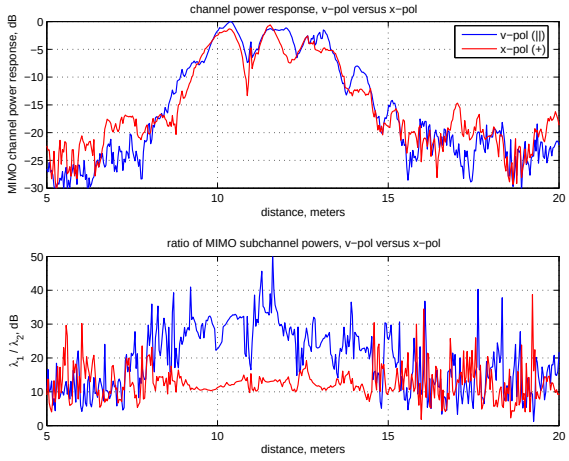

Figure 8. Example of measured MIMO radio channel, total channel power response and subchannel power ratio for two base station antenna configurations.

5.1. Frequency-Aware UL/DL Scheduling

Baseline scheduler assumes no knowledge of the instantaneous frequency response of the radio channel. For slow-moving UEs such knowledge is available at the BTS in the form of subband CQI feedback from UE. In case there is only a single user to be scheduled in downlink, it is optimal to allocate whole bandwidth, since this offers highest coding gain. In UL, the optimal bandwidth for a single simultaneous user may be less than the system bandwidth, see Fig. 2 for an example. Focusing on the downlink, in the case there are multiple simultaneous UEs to be scheduled during a TTI, the base station can schedule each UE in the frequency subband with the strongest channel power response, hence avoiding fading dips in frequency domain. This results in frequency-domain multiuser scheduling gain, which can be quantified in terms of network-level throughput gain and cell edge throughput gain.

Practical (including system imperfections) achievable downlink multiuser scheduling network-level throughput gains have been simulated to be about $< 30 - 40\%$ at network level, for $3 - 7$ users [6]. For the cell edge, throughput can be almost doubled with a suitable scheduling algorithm (always vendor-dependent). Here the gain should be interpreted relative to the throughput of a frequency-unaware scheduler with the same instantaneous number of users per TTI. Of course, even if the network-level throughput increases, actual per-user throughput will decrease when the number of simultaneous users increases.

Another benefit of the frequency-aware scheduling emerges in case the time correlation of other-cell interference power is long enough so that the scheduler has time to learn the interference spectrum and divert transmission to a cleaner part of the system bandwidth. This is only possible if UE is moving slowly and the interference is persistent in time over, say, a few dozens of TTIs. This interference rejection gain can be seen similar to what is obtained from inter-cell interference coordination, to be discussed next.

5.2. Inter-Cell Interference Coordination

There are two basic methods to coordinate frequency usage between cells in a network: static and dynamic. Static coordination means fixed allocation of frequency resources per cell over extended periods of time while dynamic frequency allocation means fast coordination within a time frame of seconds or even less, without need for manual operator intervention. In LTE, dynamic inter-cell interference coordination is inherently supported by 3GPP-specified signalling between base stations.

The network-level throughput gain from frequency use coordination is most visible with low-to-medium network load; when the network load is high no coordination will help since all frequency resources of all cells tend to be used most of the time. Hence, interference coordination is most useful for non-congested networks. Looking at Fig. 5, considerable cell edge throughput gains are possible if one can reduce the effective network load seen by the UE by allocating neighbor cell frequency resource on a different part of the system bandwidth. From Fig. 5, if the cell radius is small the throughput gain can be considerable. At network-level, throughput gains similar to channel-aware scheduling have been reported in literature for low-to-medium network loads ($\gamma < 50\%$). Summarizing, inter-cell interference coordination is mostly useful in small-range cells during off-peak hours or during early phases of network life cycle.

5.3. Uplink Fractional Power Control

LTE supports both cell-specific and UE-specific uplink power control. In LTE downlink, there is no power control in the conventional sense. With LTE power control scheme it is possible to compensate only a fraction of the path loss, reducing transmit power of cell edge UEs that generate most of the interference to other cells. This is in contrast to conventional

power control schemes that attempt to compensate path loss to the full extent allowed by the UE transmit power. The benefit of the fractional scheme is that, due to reduction in UE transmit power, network-level interference is reduced and overall UL throughput is increased. This improvement is at the expense of reduction in cell edge UL throughput. For each optimization goal - maximizing cell edge throughput or network throughput - there exist an optimum optimum power control parameter set. For early system simulation examples, see [7].

6. INTRODUCTION TO RADIO PARAMETER PLANNING

The three most important tasks in LTE prelaunch radio parameter planning are: i) Physical Cell Identity (PCI) allocation, ii) Physical Random Access Channel (PRACH) parameter planning, and iii) uplink reference signal sequence planning. Obviously, there are numerous other types of air interface parameters that can be tuned in LTE, such as UL power control and handover thresholds. However, the three tasks picked out above are the ones that must be planned before network launch, while the remaining ones can arguably be optimized also after launch, provided that reasonable default values are available. In the following, we briefly review the basics of the three main pre-launch parameter design tasks. More detailed treatment of parameter optimization and planning will be a topic of a separate exposition.

6.1. PCI planning

In LTE, Physical Cell Identity (PCI) allocation is a task somewhat similar to scrambling code allocation in WCDMA. PCI is encoded in the physical layer synchronization signal transmission and is used by the UE for neighbour cell handover measurement reports. Hence, as in WCDMA, the PCI should uniquely identify the neighbouring cell to the serving eNB, within a certain geographical area. Consequently, PCI reuse distance should be large enough so that UE cannot measure and report two cells with the same PCI. This part of the PCI allocation should not pose a problem since there are 504 PCIs defined.

The second, perhaps less obvious, purpose of the PCI is to serve as a resource allocator parameter for downlink and uplink Reference Signals (RS).

DL Reference Signal: Downlink reference symbols ("LTE pilot signal") are allocated in a time-frequency grid as shown in Fig. 9. The figure illustrates three frame-synchronized cells with PCIs 9, 10, and 11. For example, these could represent different cells of the same eNB site[6]. In time domain the RS are always transmitted in the same OFDM symbol. However, in frequency domain each cell has a different shift determined by modulo-3 of the PCI, denoted $\mathrm{PCI} \bmod 3$. In Fig. 9, cell #1 has $\mathrm{PCI} \bmod 3 = 0$, cell #2 has $\mathrm{PCI} \bmod 3 = 1$, while cell #3 has $\mathrm{PCI} \bmod 3 = 2$. With this PCI allocation, the RS of different cells do not overlap in frequency, which results in less interference on UE channel estimation. If neighbouring sites are frame-synchronized (e.g., using GPS), or the frame timing offset between sites is known, the PCI allocation should also be coordinated between neighbouring sites, which brings additional complexity in the allocation process. On the other hand, if the neighbouring sites are not frame-synchronized or the frame timing offset is not known (i.e., random), one cannot coordinate PCI allocation between sites.

It should be noted that assigning PCIs as shown in Fig. 9 results in RS overlapping with the control and data Resource Elements of the neighbouring cells. Therefore, a design choice must be made between RS$\leftrightarrow$RS interference and RS$\leftrightarrow$PDSCH/PDCCH intererence. The current engineering consensus seems to be that the latter choice is favoured, due to the fact that if two frame-synchronized cells have the same

[6]Note that Fig. 9 shows transmission of both transmit antennas in the same grid, to save space. Frame synchronization in this context means that the DL transmission of a radio frame starts at the same time instant in all three cells.

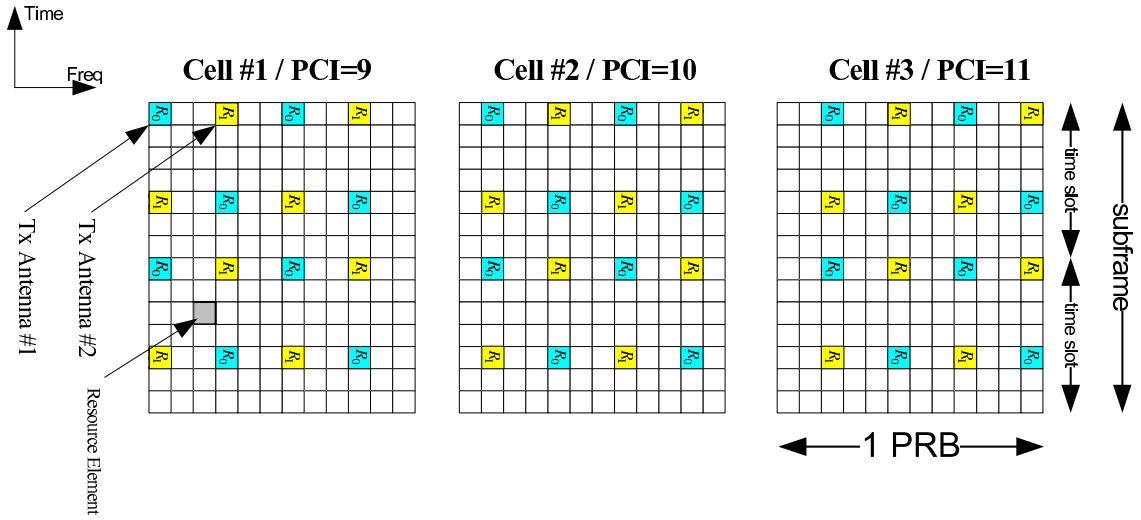

Figure 9. Location of Reference Symbols within one PRB for different PCIs. Frame-synchronized cells shown.

PCI mod 3, the additional drawback is that their Primary Synchronization Signals will interfere with each other, causing problems in cell search and handover measurements.

UL Reference Signal: LTE uplink shared data channel (PUSCH) carries Demodulation Reference Signal (DM RS). Optionally also Sounding Reference Signal is transmitted in the uplink. The uplink DM RS are constructed from Zadoff-Chu sequences which are divided into 30 groups. Roughly, this means that for a given number of PRBs allocated in the uplink there are 30 different base sequences that can be used as the reference signal[7]. The cross-correlation between the base sequences is on average low, which is beneficial from inter-cell interference point of view. It follows that the planning requirement is that the neighbouring cells should be allocated different base sequences. The simplest method is to ensure that PCI mod 30 of potentially interfering cells is different. This is because in the simplest scheme the DM RS base sequence index is equal to $u =$PCI mod 30, where $u = 0 \ldots 29$ is the base sequence index. An example of this simple PCI-based DM RS sequence allocation scheme is shown in Fig. 10. In practical network deployments this simple planning criterion cannot be always fulfilled. As a remedy to such a case, there are additional sequence allocation schemes built-in in the 3GPP specification, most notably a static base sequence index offset parameter, DM RS cyclic shift planning, and pseudo-random base sequence hopping ("u-hopping"). These will be discussed next.

[7]There are actually two groups of 30 sequences defined for PRB allocations of 6 or more. These can be pseudo-randomly alternated. However, this option is not considered in this paper.

6.2. UL Reference Signal sequence planning

The simple PCI-based based sequence uplink DM RS allocation scheme from the previous section may be difficult to plan since the same base sequence is reused in every 30th cell, which may lead to insufficient cell separation.

There are three options to reduce uplink inter-cell interference in such cases:

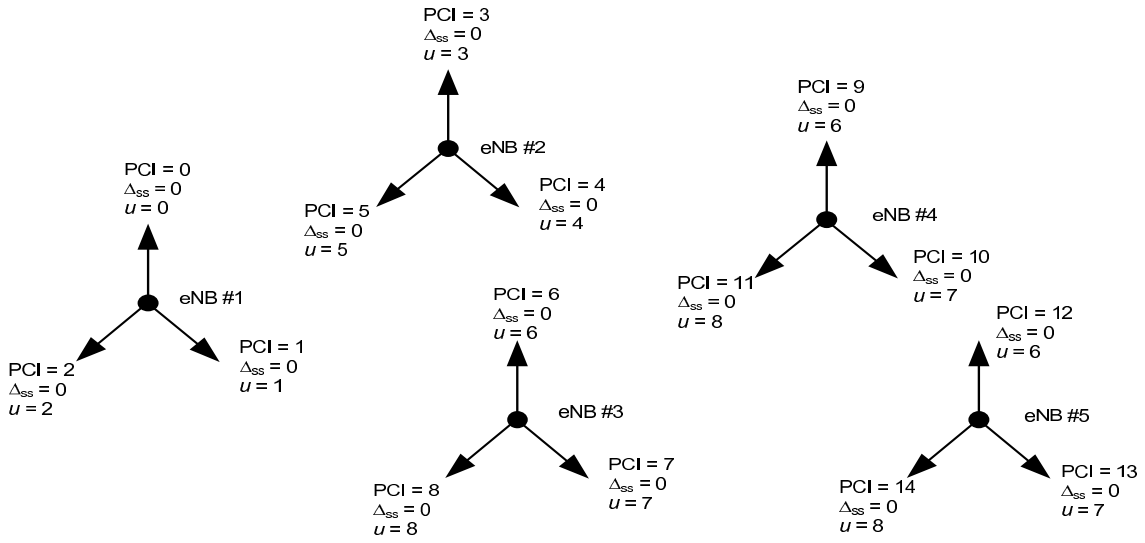

Figure 10. Simple PCI-based uplink DM RS allocation scheme. Different base sequence u allocated to every cell based on PCImod30, every cell has $\Delta_{ss} = 0$.

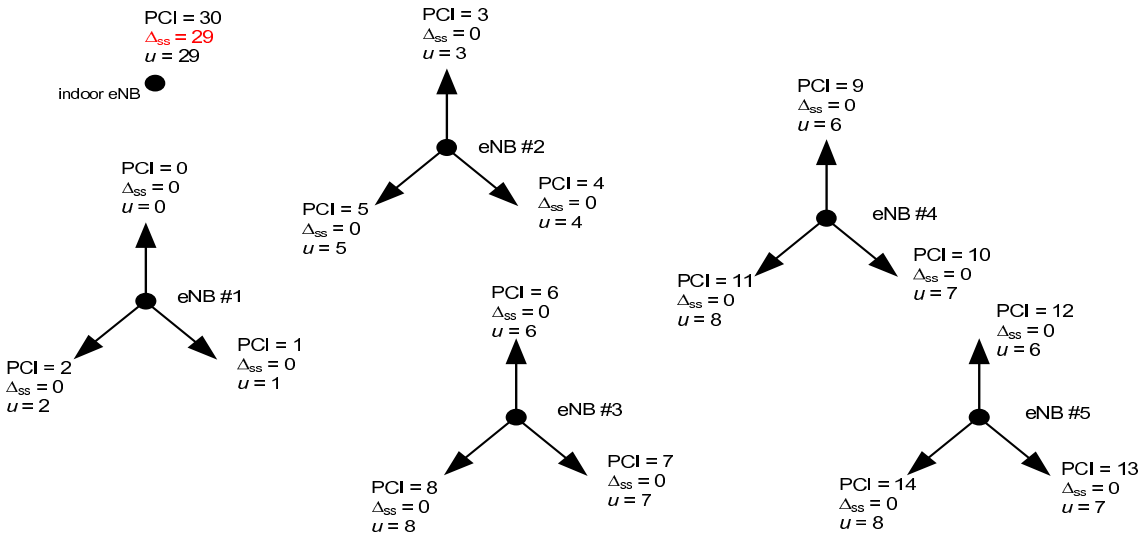

Figure 11. Example of how the parameter Δ_{ss} can a base sequence collision between two cells. The indoor cell has been allocated PCI=30 which would result in $u = 0$ if $\Delta_{ss} = 0$, hence creating UL interference with cell PCI=0. Setting $\Delta_{ss} = 29$ gives $u = (30 + 29) \bmod 30 = 29$ instead.

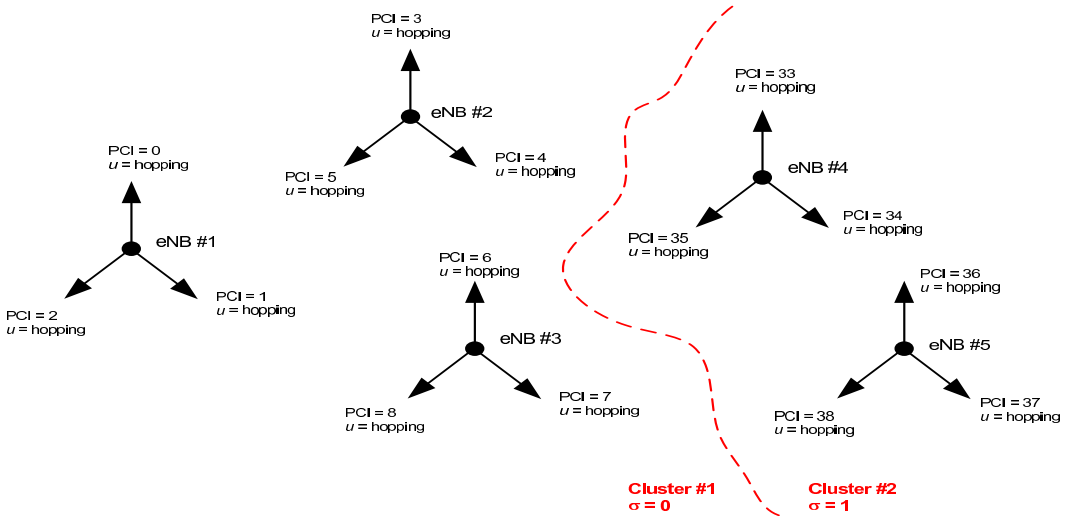

Figure 12. Example of u-hopping. Cluster #1 has hopping-pattern $\sigma = 0$ and cluster #2 has hopping-pattern $\sigma = 1$. Sequence offset $\Delta_{ss} = 0$ for all cells. Systematic base sequence collisions within a group are avoided within a group. Random base sequence collisions are possible in the cluster border.

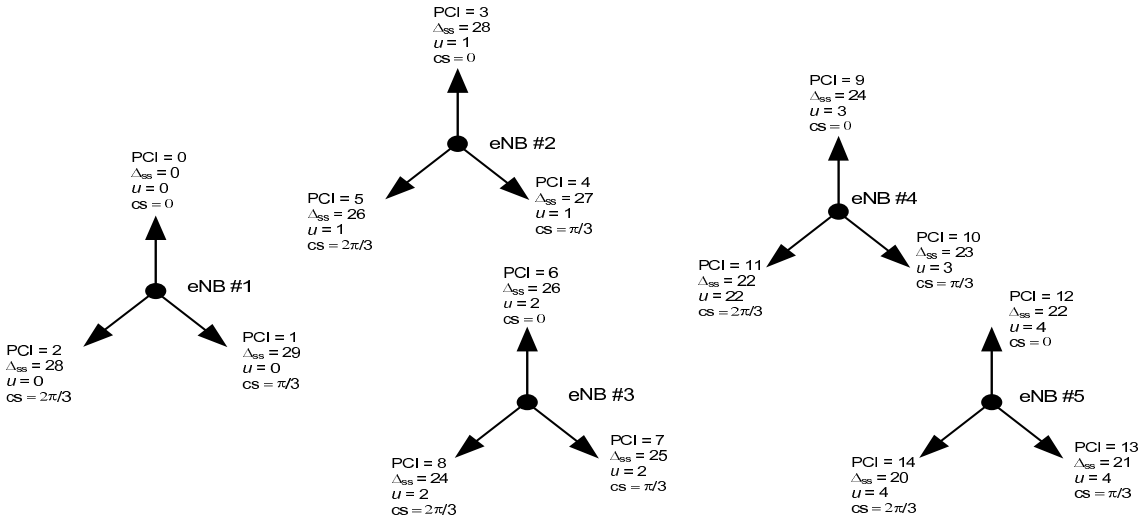

Figure 13. Example of cyclic shift planning. Cells of the same site are allocated the same base sequence u using the offset parameter Δ_{ss}. Inter-cell interference between cells of the same site is mitigated by setting different cell-specific cyclic shift (cs) for cells of a site.

- Bypass the simple PCI-based base allocation scheme by explicitly defining the base sequence used in the cell. This brings additional flexibility to base sequence allocation, and effectively decouples the PCI planning from uplink DM RS base sequence planning.
- The base sequence u can change pseudo-randomly for every 0.5ms time slot. This planning option randomizes base sequence collisions and averages inter-cell interference.
- Different cyclic shifts of a ZC sequence are orthogonal. This can be utilized by assigning a different cyclic shift on two cells that use the same base sequence u. The cell-specific static cyclic shift is broadcasted on BCCH.

Defining u independently from PCI: The simplest scheme assigns the base sequence index u to a cell as modulo-30 of PCI. Optionally, the base sequence can be assigned to a cell as

$$u = (PCI + \Delta_{ss}) \bmod 30\,,$$

where $\Delta_{ss} = 0 \ldots 29$ is an offset parameter signalled on BCCH. In the simple PCI-based scheme $\Delta_{ss} = 0$. With Δ_{ss} it is possible to avoid collisions in cells that would otherwise use the same u due to PCI allocation. An example of Δ_{ss} planning is shown in Fig. 11.

Pseudo-random u-hopping: If u-hopping is activated, the base sequence used in the cell changes at every time slot in a pseudo-random fashion. The index of base sequence in time slot n [8]

$$u_n = (\nu_n + PCI + \Delta_{ss}) \bmod 30\,,$$

where $\nu_n = 0 \ldots 29$ is pseudo-random integer defined by the hopping-pattern. The hopping pattern defined used in a cell is defined by the index $\sigma = \lfloor \frac{PCI}{30} \rfloor$. Thus, there are 17 u-hopping patterns defined since there are 504 PCIs defined, i.e., $\sigma = 0 \ldots 16$. A foreseen method of PCI planning, where near-by cells are assigned near-by PCI values, results in grouping of cells into "clusters-of-30", where within each cell cluster the same hopping-pattern is used. To prevent systematic collisions, static part of the sequence group assignment, $(PCI + \Delta_{ss})$ mod 30, should be different, especially for frame-synchronized cells. At the border of two cell clusters having different σ, random sequence group collisions are possible since two different hopping patterns are utilized. An example of this planning scheme is shown in Fig. 12.

Cyclic shift planning: So far we have considered only how to reduce inter-cell interference by assigning different base sequences to every neighbouring cell. Another interference reduction method follows from the fact that ZC sequences have the useful property that two different cyclic shifts of the same base sequence are orthogonal[9]. Therefore, if a pair of cells have been allocated the same base sequence u, inter-cell interference can be reduced by assigning a different cyclic shift to the cells. This scheme can be applied to cells of one site as shown in Fig. 13. Other applications, tangential to our present discussion, are uplink multi-user MIMO (where each UE uses a different cyclic shift) and, in LTE-A, uplink single-user MIMO (where each UE transmit antenna uses a different cyclic shift), or a combination of the two. It should be noted that cyclic shift planning can also be combined with the other two schemes discussed in this section.

6.3. PRACH parameter planning

The random access procedure in LTE uplink begins when UE transmits a preamble to the eNB. The specific preamble is selected randomly by UE from a pre-defined set of 64 Zadoff-Chu sequences. To avoid call setup anomalies, each cell (within a reuse distance) has its own unique set of 64 preambles, and the information of the

[8] There are 20 time slots in a radio frame. The hopping pattern is re-initialized at the beginning of every radio frame.

[9] Cyclic shifts of extended ZC sequences used in uplink DM RS are not orthogonal, however.

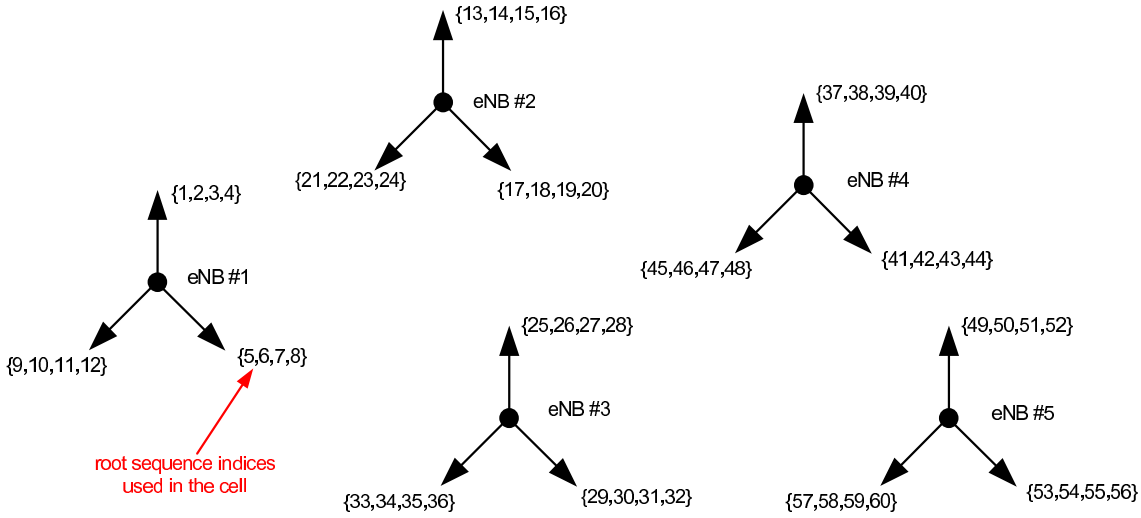

Figure 14. Example of root sequence allocation for different cells. Four sequences per cell are allocated, PRACH configuration index = 8, see Table 3.

specific set to use in the cell is broadcasted on BCCH. The preamble sequence allocation depends on cell range: for example, if one (unrealistically) requires that all cells must be accessible from 100km away then there would be only a total of 839 preamble sequences available. As each cell must have exactly 64 preambles, the total number of cells within a reuse distance would then be only $\frac{839}{64} \approx 13$, and in this case each cell consumes 64 ZC sequences (one full ZC sequence per preamble) out of the total of 839 ZC sequences available for PRACH. More sequences can be generated if the "random access radius" of cells is dimensioned more realistically; continuing the example, if maximum random access cell range is chosen as 1km, one ZC sequence generates 64 preambles, instead of the one preamble in the 100km case. Summarizing, the PRACH parameter planning task consists of deciding i) the maximum cell range for random access, and ii) allocating the ZC sequences to cells.

Table 3 lists the number of ZC sequences required per cell, for a given random access radius. One can see that a cell requires five ZC sequences per cell for up to 7.3km radius, which is typically sufficient for urban and suburban macro cells. This results in sequence reuse factor of at least $839/5 \approx 167$ cells, hence allows for easy planning process. Example of root sequence allocation is shown in Fig. 14. The point to notice here is that root sequence indices of cells must not overlap within the reuse distance[10]. As for typical scenarios there are plenty of ZC sequences available, for safety margin and ease of planning one can overdimension the random access radius of the cells in a given planning region, to simplify allocation. In the example of Fig. 14 each cell consumes four sequences, corresponding to maximum radius of 5.4km for every cell.

If root sequences used in neighbouring cells overlap, the transmitted preamble may be de-

[10]To reduce signalling load, only the index of the first root sequence used in the cell and the PRACH configuration index is transmitted on BCCH.

tected in multiple cells. The drawback are the "ghost" preambles which consequently result in unnecessary PDCCH and PUSCH resource reservation in those cells that whose random access responses the UE chooses to neglect[11].

Table 3
PRACH ZC sequence parameters from the 3GPP specification.

PRACH configuration index	Number of root sequences per cell	Random access radius [km]⋆
1	1	0.7
2	2	1
3	2	1.4
4	2	2
5	2	2.5
6	3	3.4
7	3	4.3
8	4	5.4
9	5	7.3
10	6	9.7
11	8	12.1
12	10	15.8
13	13	22.7
14	22	38.7
15	32	58.7
0	64	118.8

⋆ Includes 1.2μsec implementation margin for delay estimation

7. CONCLUSION

In this paper topics related to radio planning in LTE were discussed. Besides the link budget for coverage and interference-limited cases, the tradeoff between cell range, cell edge throughput and network load was discussed under uncoordinated interference. Impact of MIMO and antenna configurations was illustrated using a measurement example. Finally, some advanced radio resource management features and detailed radio parameter planning tasks were introduced.

[11]Similar problem exists in GSM networks where ghost random accesses result in unnecessary SDCCH reservation.

REFERENCES

1. H. Holma *et al* (eds.), LTE for UMTS, Wiley, 2009.
2. F. Khan, LTE for 4G Mobile Broadband, Cambridge University Press, 2009.
3. S. Sesia *et al* (eds.), LTE, The UMTS Long Term Evolution: From Theory to Practice, Wiley, 2009.
4. 3GPP TS 25.814, v7.1.0, 2006.
5. P. Suvikunnas *et al*, Comparison of MIMO Antenna Configurations: Methods and Experimental Results, IEEE Trans VT, 2008
6. A. Pokhariyal *et al*, Frequency Domain Packet Scheduling Under Fractional Load for the UTRAN LTE Downlink, IEEE VTC, 2007
7. C. U. Castellanos *et al*, Performance of Uplink Fractional Power Control in UTRAN LTE, IEEE VTC, 2008.

Jari Salo received the degrees of Master of Science in Technology and Doctor of Science in Technology from Helsinki University of Technology (TKK) in 2000 and 2006, respectively. Since 2006, he has been with European Communications Engineering Ltd, where he works as a consultant for mobile wireless industry and operators. His present interest is in radio and IP transmission planning and optimization for wireless networks. He has written or co-written 14 IEE/IEEE journal papers, 35 conference papers, and is the recipient of the Neal Shepherd Memorial Best Propagation Paper Award from the IEEE Vehicular Technology Society, for the best radio propagation paper published in IEEE Transactions on Vehicular Technology during 2007. He is also a co-creator of the wide-band spatial channel model adopted by 3GPP for LTE system-level simulations. *E-mail: jari.salo@eceltd.com*

Mohammad Nur-A-Alam obtained his Master of Science degree from Tampere University of Technology (TUT) in 2009 and is currently working towards Ph.D in the same department. After attaining his BSc. in Electrical and Electronic Engineering from Islamic University of Technology in 2003, he worked in Telecom Malaysia International as a Network Planning and Optimization Engineer. From 2008 to 2010, he was with ECE Ltd as LTE Consultant. He is currently working for Nokia Siemens Networks as system solution manager and his interest are in LTE/HSPA+ radio network planning.

Kwangrok Chang received the degrees of Master and Ph.D in Electronic and Electrical Engineering from POSTECH (Pohang University of Science and Technology) in 1995 and 1998, respectively. In July of 1998 he joined LG Electronics Ltd for two years, after which he has been with Nokia Siemens Networks Ltd., where he is currently heading the Network Planning and Optimization Group of Japan and Korea. His present interests are network capacity management and enhancement of end user performances in high speed data networks, such as HSPA, and network planning/dimensioning of LTE system.